nature genetics

© 2008 Nature Publishing Group http://www.nature.com/naturegenetics

Pathological responses to oncogenic Hedgehog signaling in skin are dependent on canonical Wnt/β-catenin signaling

Steven Hoseong Yang[1,2], Thomas Andl[3,5], Vladimir Grachtchouk[1,5], Aiqin Wang[1], Jianhong Liu[1], Li-Jyun Syu[1], Jenny Ferris[1], Timothy S Wang[1], Adam B Glick[4], Sarah E Millar[3] & Andrzej A Dlugosz[1,2]

Constitutive Hedgehog (Hh) signaling underlies several human tumors[1], including basal cell carcinoma (BCC) and basaloid follicular hamartoma in skin[2,3]. Intriguingly, superficial BCCs arise as *de novo* epithelial buds resembling embryonic hair germs[4–6], collections of epidermal cells whose development is regulated by canonical Wnt/β-catenin signaling[7,8]. Similar to embryonic hair germs, human BCC buds showed increased levels of cytoplasmic and nuclear β-catenin and expressed early hair follicle lineage markers. We also detected canonical Wnt/β-catenin signaling in epithelial buds and hamartomas from mice expressing an oncogene, *M2SMO*[9], leading to constitutive Hh signaling in skin. Conditional overexpression of the Wnt pathway antagonist Dkk1 in M2SMO-expressing mice potently inhibited epithelial bud and hamartoma development without affecting Hh signaling. Our findings uncover a hitherto unknown requirement for ligand-driven, canonical Wnt/β-catenin signaling for Hh pathway-driven tumorigenesis, identify a new pharmacological target for these neoplasms and establish the molecular basis for the well-known similarity between early superficial BCCs and embryonic hair germs.

Hair follicle development is orchestrated by secreted signaling molecules that act on intracellular effector pathways in epithelial and mesenchymal progenitors[10]. The canonical Wnt signaling pathway initiates hair bud formation, whereas Hh signaling subsequently promotes the proliferative expansion of follicle epithelium required to assemble a mature follicle[7,8,11,12]. BCC is the most common type of cancer in light-skinned individuals, and several mutations leading to constitutive activation of the Hh pathway have been identified in these tumors, including loss-of-function mutations in *PTCH1* and gain-of-function mutations in *SMO*[2]. Nearly all human BCCs show elevated Hh pathway activity, and several animal models support the notion that uncontrolled Hh signaling is sufficient to drive BCC- or BCC-like tumorigenesis in mice[2]. The morphological similarity between early superficial BCCs and hair germs was first noted over 70 years ago[4,5], suggesting the possibility that canonical Wnt signaling is involved in pathological responses to deregulated Hh signaling in skin. Although some prior studies have identified coordinate changes in the Hh and canonical Wnt pathways in BCCs and other neoplasms[13–19], direct evidence establishing the functional significance of Wnt signaling in Hh pathway-driven pathology *in vivo* is lacking. In this report we combined analysis of human tissues with in-depth studies of genetic mouse models to test the role of Hh-Wnt crosstalk in the setting of constitutive Hh signaling in skin.

Both human superficial BCCs and embryonic hair buds (**Fig. 1**) comprise a focal grouping of epidermal cells protruding into the underlying dermis (**Fig. 1a**,**b**) and express early-stage follicle lineage markers, including the outer root sheath markers K17 and Sox9, and the hair matrix/inner root sheath marker CDP (**Fig. 1c**,**d**,**g–j**). Epithelial cells in both the superficial BCCs and embryonic hair buds were more proliferative, based on Ki67 immunostaining, than adjacent epidermis (**Fig. 1k**,**l**) and did not express the epidermal differentiation marker K1 (**Fig. 1e**,**f**). In contrast to embryonic hair buds (**Fig. 1b**, arrowhead), superficial BCCs did not show a morphologically recognizable mesenchymal papilla (**Fig. 1a**), which is required for later stages of hair follicle morphogenesis.

We then examined epithelial bud development in mice with focally activated Hh signaling in skin, achieved using the *M2SMO* oncogene[9] (**Fig. 2**). We restricted much of our analysis to a triangular region of volar skin completely devoid of follicles or other skin appendages, allowing us to study the effects of deregulated Hh signaling in a morphogenetically naive epidermis (**Fig. 2a**). Constitutive activation of Hh signaling using M2SMO resulted in *de novo* epithelial bud initiation in this normally hairless region (**Fig. 2b–e**). Similar to

[1]Department of Dermatology and Comprehensive Cancer Center and [2]Graduate Program in Cellular and Molecular Biology, University of Michigan Medical School, 1500 East Medical Center Drive, Ann Arbor, Michigan 48109, USA. [3]Departments of Dermatology and Cell and Developmental Biology, University of Pennsylvania School of Medicine, 422 Curie Boulevard, Philadelphia, Pennsylvania 19104, USA. [4]Department of Veterinary and Biomedical Sciences, Center for Molecular Toxicology and Carcinogenesis, Pennsylvania State University, University Park, Pennsylvania 16802, USA. [5]Present addresses: Department of Medicine, Vanderbilt University Medical Center, 1161 21st Avenue South, Nashville, Tennessee 37232, USA (T.A.) and Department of Cell Stress Biology, Roswell Park Cancer Institute, Elm and Carlton St., Buffalo, New York 14263, USA (V.G.). Correspondence should be addressed to A.A.D. (dlugosza@umich.edu).

Received 9 April; accepted 6 June; published online 1 August 2008; doi:10.1038/ng.192

© 2008 Nature Publishing Group http://www.nature.com/naturegenetics

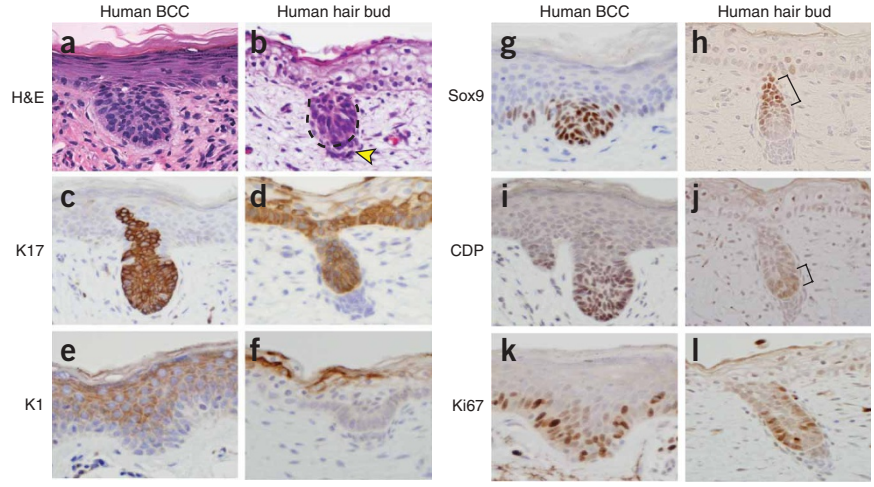

Figure 1 Human superficial basal cell carcinoma (BCC) expresses hair bud lineage markers. (**a**,**b**) H&E-stained sections of early human superficial BCC and embryonic hair buds. Dashed line in **b** indicates epithelial component of embryonic hair follicle, with adjacent mesenchymal condensate marked with an arrowhead. Note absence of morphologically recognizable mesenchymal condensate near superficial BCC. (**c**,**d**) Hair placode marker K17 is expressed in superficial BCC and hair bud. At this stage of embryonic development, surrounding epidermis (**d**) also expresses this marker. (**e**,**f**) The suprabasal cell marker K1 is not expressed in superficial BCC or in hair bud. (**g**–**j**) Outer root sheath marker Sox9 and hair matrix/inner root sheath marker CDP are expressed in superficial BCC and hair bud. Note largely nonoverlapping expression patterns of Sox9 and CDP in hair bud (brackets in **h** and **j**), as compared with overlapping expression in superficial BCC. (**k**,**l**) Increased proliferation in superficial BCC and hair bud relative to adjacent epidermis, assessed by Ki67 staining.

human superficial BCC and embryonic hair germs (**Fig. 1**), immunophenotyping revealed multiple similarities between M2SMO-induced epithelial buds and embryonic mouse hair buds (**Fig. 2h–u**). However, downregulation of E-cadherin, a characteristic alteration in embryonic hair buds that may contribute to a shift from membrane-bound to cytoplasmic and nuclear β-catenin, was not apparent in M2SMO-induced buds (**Fig. 2v**,**w**), and M2SMO-induced ectopic buds (like human superficial BCCs) were not associated with a morphologically or biochemically detectable mesenchymal condensate (**Fig. 2g**,**h**).

The formation of *de novo* epithelial buds in response to ectopic Hh signaling in epidermis was intriguing, given the compelling evidence pointing to the canonical Wnt pathway as the initiator of skin appendage development[7,8,20–22]. We therefore determined whether pathological Hh signaling in this setting was associated with activation of the canonical Wnt/β-catenin pathway (**Fig. 3**). Increased levels of β-catenin in the cytoplasm and nucleus were seen in human embryonic hair buds (**Fig. 3b**), consistent with the notion that Wnt/β-catenin signaling is activated during early stages of human follicle development, as already shown in mouse hair follicles (**Fig. 3d**). We also detected increased levels of β-catenin in the cytoplasm and nucleus of neoplastic cells in human superficial BCCs and in M2SMO-induced mouse epithelial buds (**Fig. 3a**,**c**), suggesting activation of the canonical Wnt pathway in response to ectopic Hh signaling. Furthermore, nonphosphorylated (active) β-catenin was detected in lysates from *M2SMO*-transgenic mouse skin by immunoblotting, with little or no expression in control, nontransgenic volar

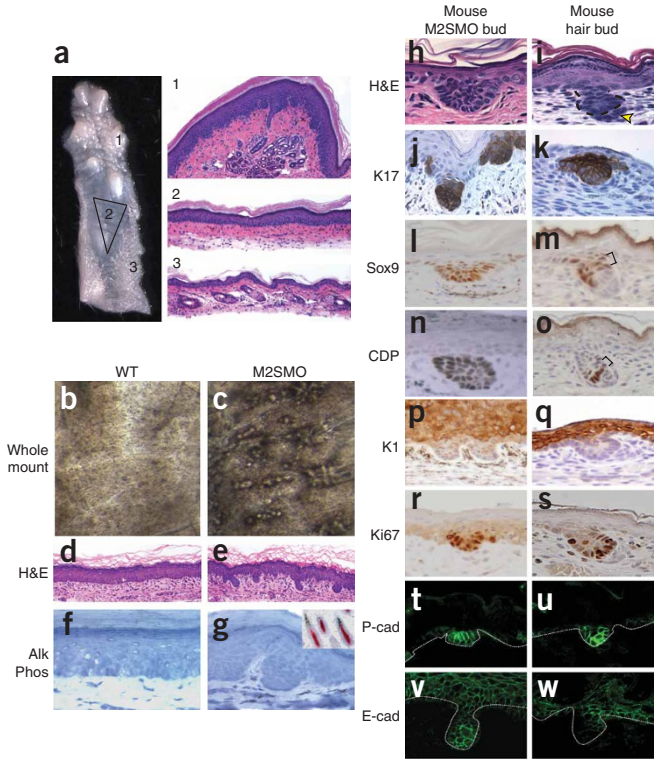

Figure 2 Ectopic Hh signaling in M2SMO-expressing hairless mouse skin drives superficial BCC-like downgrowths resembling hair buds. Histological appearance, marker expression and increased proliferation rate of ectopic epithelial buds in volar skin from M2SMO-expressing mice and hair bud from embryonic day 16.5 mouse embryo. (**a**) Whole-mount view of control skin from ventral aspect of mouse hind limb, with H&E-stained sections from indicated regions. Triangle outlines a region completely devoid of hair follicles or other skin appendages (2), compared to eccrine glands in the footpad region (1) and hair follicles at the periphery (3). (**b**,**c**) Whole-mount view of hairless control (WT) and *M2SMO*-transgenic volar skin. Activation of Hh signaling using M2SMO results in the appearance of scattered buds and hyperpigmentation in hairless skin (**c**). (**d**,**e**) H&E-stained sections showing distribution of buds in M2SMO volar skin (**e**). (**f**,**g**) Endogenous alkaline phosphatase (Alk Phos), a marker for follicle-associated mesenchymal condensates, is not detected in control or M2SMO volar skin. Inset in **g** shows alkaline phosphatase–positive (red) dermal papillae in hair follicles. (**h**,**i**) H&E-stained sections of *de novo* epithelial bud in M2SMO volar skin and embryonic mouse hair bud. The mesenchymal condensate neighboring normal hair buds (arrowhead in **i**) is not detected in association with the M2SMO-induced bud (**h**). Immunostaining revealed expression of hair follicle outer root sheath markers K17 and Sox9 (**j**–**m**), and the hair matrix/inner root sheath marker CDP (**n**,**o**) in ectopic buds and embryonic hair buds. Note nonoverlapping expression of Sox9 and CDP in hair buds (brackets in **m** and **o**), as compared with M2SMO-induced bud. (**p**,**q**) The suprabasal marker K1 is not expressed in M2SMO-induced buds or embryonic hair buds, whereas proliferation (**r**,**s**) is increased in both. (**t**,**u**) The hair bud marker P-cadherin (P-cad) is upregulated in both M2SMO and embryonic hair buds, whereas downregulation of E-cadherin (E-cad) is detected only in hair buds (**v**,**w**). White dotted line shows epidermal-dermal junction.

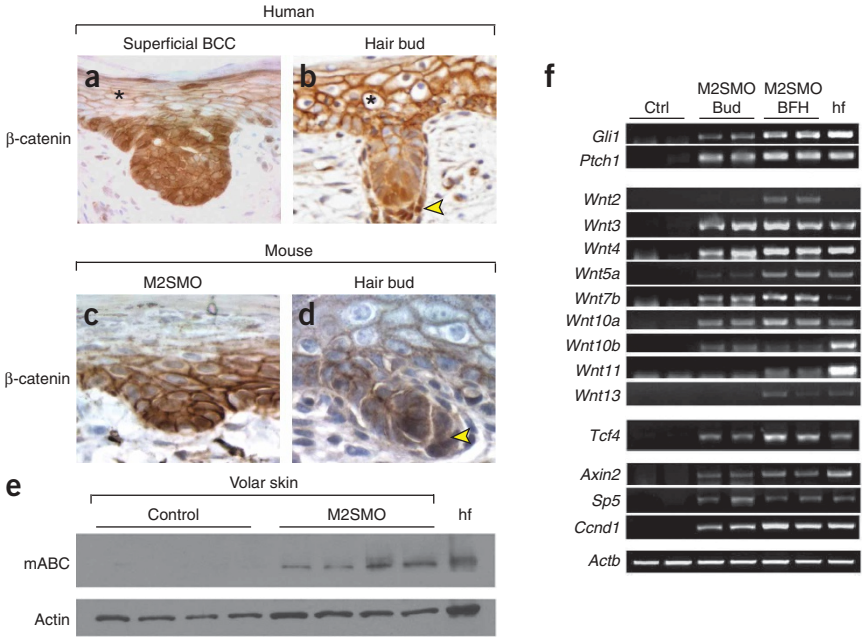

Figure 3 Canonical Wnt signaling is activated in human superficial BCC and epithelial buds in M2SMO-expressing hairless mouse skin. (**a**,**b**) β-catenin immunostaining reveals nuclear-cytoplasmic β-catenin localization in human superficial BCC and hair bud, consistent with activation of canonical Wnt signaling. Note intense nuclear staining in mesenchymal cells adjacent to hair bud (arrowhead in **b**) but not BCC (**a**). Adjacent epidermis (*) exhibits β-catenin localized to the cell membrane. (**c**,**d**) Similarly, β-catenin immunostaining reveals nuclear-cytoplasmic localization in mouse M2SMO bud cells arising from hairless volar skin and embryonic day 16.5 mouse embryonic hair bud, with stained mesenchymal cells also noted adjacent to the hair bud (arrowhead). (**e**) Immunoblotting using mouse ABC antibody showing presence of nonphosphorylated (active) β-catenin in lysates from M2SMO volar skin, but not hairless control volar skin. Skin lysate from postnatal day 8 mouse with actively growing hair follicles (hf) was used as a positive control. (**f**) Semiquantitative RT-PCR was performed on RNA isolated from control volar skin (Ctrl), early bud-stage *M2SMO*-transgenic volar skin (M2SMO Bud) and later, basaloid follicular hamartoma-containing (**Supplementary Fig. 1**) M2SMO volar skin (M2SMO BFH), with postnatal day 8 skin as a positive control (hf). Upregulation of *Gli1* and *Ptch1* expression in M2SMO skin confirms activation of Hh signaling. M2SMO-expressing skin expresses multiple Wnt genes, *Tcf4* and endogenous Wnt target genes *Axin2*, *Sp5* and *Ccnd1*. In control volar skin there is negligible expression of *Gli1*, *Ptch1* and Wnt pathway-associated genes.

skin (**Fig. 3e**). Epithelial buds arising in M2SMO-expressing mice progress to form follicular hamartomas (**Supplementary Fig. 1** online), a type of benign tumor associated with deregulated Hh signaling in mice and humans[3,23,24], but not BCCs. Follicular hamartomas expressed the same set of lineage markers as buds, but with Ki67, β-catenin and cyclin D1 largely restricted to the outermost cell layers (**Supplementary Fig. 1** and **Supplementary Note** online).

To determine whether aberrant Hh signaling may be influencing the canonical Wnt/β-catenin pathway through alterations in Wnt ligand expression, we performed semiquantitative reverse transcriptase–polymerase chain reaction (RT-PCR) (**Fig. 3f**). As expected, mRNA encoding the Hh target genes *Gli1* and *Ptch1*, indicating Hh pathway activation, was detected in samples from M2SMO volar skin, with negligible levels in controls. In addition, transcripts encoding multiple Wnt ligands (Wnt3, 4, 5a, 7b, 10a and 10b) and the transcriptional coactivator Tcf4, were coordinately induced in M2SMO volar skin. Expression of endogenous Wnt target genes[25] *Axin2* and *Sp5*, and the indirect target *Ccnd1*, was also upregulated in M2SMO-expressing skin, indicating activation of a transcriptional program associated with canonical Wnt signaling.

Using a transgenic mouse model wherein doxycycline-regulated activation of the secreted Wnt inhibitor Dkk1 could be achieved in skin[26], we next tested whether canonical Wnt signaling was required for development of epithelial buds and their expansion to form hamartomas (**Fig. 4**). We first induced Dkk1 in M2SMO-expressing mice (M2SMO + Dkk1) during embryogenesis by administering doxycycline to pregnant dams at embryonic day 16.5 (**Fig. 4a**). Blockade of canonical Wnt signaling at this stage led to nearly complete inhibition of M2SMO-driven ectopic bud development in volar skin, as assessed by whole-mount analysis and histology (**Fig. 4b**) of skin on postnatal day 7 (P7). Dkk1 induction at P1 (**Fig. 4c**) also led to a marked inhibition of M2SMO-mediated hair bud development and a profound suppression of follicular hamartoma formation, both in volar (**Fig. 4d**) and in tail (**Fig. 4e**) skin examined at P35. Although expression of *Wnt* genes was similarly elevated in M2SMO and M2SMO + Dkk1 skin (**Fig. 4g**), translocation of β-catenin to the cytoplasm and nucleus was suppressed in M2SMO + Dkk1 mice (**Fig. 4f**), and expression of the Wnt target genes *Axin2* and *Sp5* was negligible, indicating effective blockade of canonical Wnt signaling by Dkk1 (**Fig. 4g**). In contrast, expression of the Hh target genes *Gli1* and *Ptch1* was similar in M2SMO and M2SMO + Dkk1 skin, indicating that M2SMO-driven constitutive Hh signaling was unaffected by Wnt pathway inhibition (**Fig. 4g**). Similarly, ectopic expression of the Hh-responsive keratin, K17 (ref. 27) was seen in both M2SMO and M2SMO + Dkk1 volar skin (**Fig. 4h**), whereas expression of hair bud and follicular hamartoma markers Sox9 and CDP, and increased cell proliferation, were no longer detected in M2SMO + Dkk1 mice (**Fig. 4h**). The profound blockade of M2SMO-induced hair bud and follicular hamartoma development by Dkk1 establishes that biological responses to ectopic Hh signaling in skin are largely mediated indirectly, via the canonical Wnt/β-catenin signaling pathway.

Notably, buds and hamartomas also developed in dorsal skin of M2SMO mice, but in this location they were not suppressed in M2SMO + Dkk1 mice, and β-catenin remained localized to the nucleus, suggesting that Dkk1 was not effectively inhibiting canonical Wnt signaling at this site. This may be due to insufficiently high expression of Dkk1 in dorsal skin or a relative deficiency in the level of Kremens 1 and 2 (ref. 28), which facilitate Dkk1's ability to block Wnt signaling. Bud and hamartoma development was also not inhibited in small regions of volar skin near footpads (arrowhead in **Fig. 4d**), and here again the presence of nuclear β-catenin indicated inefficient blockade of canonical Wnt signaling. These results further underscore the tight correlation between inhibition of canonical Wnt/β-catenin signaling and suppression of Hh pathway-induced bud and hamartoma development.

© 2008 Nature Publishing Group http://www.nature.com/naturegenetics

There are multiple reports describing interactions between the Wnt and Hh pathways at various levels, and two of these are particularly noteworthy in light of our findings. Expression of *Wnt5A*, *7B*, *7C*, *8*, *8B* and *11* has been reported in *Xenopus* animal cap explants injected with Gli2 and Gli3 mRNA, and blockade of Wnt signaling inhibits the morphogenetic response to Gli2 in this system[15]. Also, in E1A-immortalized RK3E rat kidney cells, expression of *Wnt2b*, *Wnt4* and *Wnt7* was induced by GLI1, and dominant-negative TCF4 inhibited GLI1-mediated focus formation in cell culture[19]. Although these data demonstrate that Hh-Wnt crosstalk is necessary for an embryonic process and *in vitro* transformation, respectively, our findings are the first to establish a stringent requirement for canonical Wnt/β-catenin signaling in Hh pathway-driven neoplasia.

Previous studies in normal skin have shown that in developing hair buds, canonical Wnt signaling precedes, and is required for, subsequent activation of Hh signaling[7,8,20,21]. Our data indicate that this temporal relationship is reversed in the setting of Hh-driven pathology in epidermis, where ectopic activation of Hh signaling leads to canonical Wnt signaling with resultant formation of *de novo* epithelial buds and follicular hamartomas. Several earlier reports have described links between the Hh and Wnt pathways in BCC, including upregulation of one or more Wnt genes[15] and localization of β-catenin to the cytoplasm and/or nucleus[16–18]. Our results are in keeping with these observations and provide the first direct evidence that canonical Wnt signaling is essential for a tumorigenic response to deregulated Hh signaling in skin, but additional studies are required to test the importance of Hh-Wnt cross-talk in full-blown BCC. Interestingly, a recent report described a role for β-catenin in cutaneous squamous cell carcinoma[29], which is biologically and pathogenetically distinct from BCC and follicular hamartomas, and not linked to aberrations in the Hh pathway, but it is not known whether signaling in squamous tumors is driven by Wnt ligands.

© 2008 Nature Publishing Group http://www.nature.com/naturegenetics

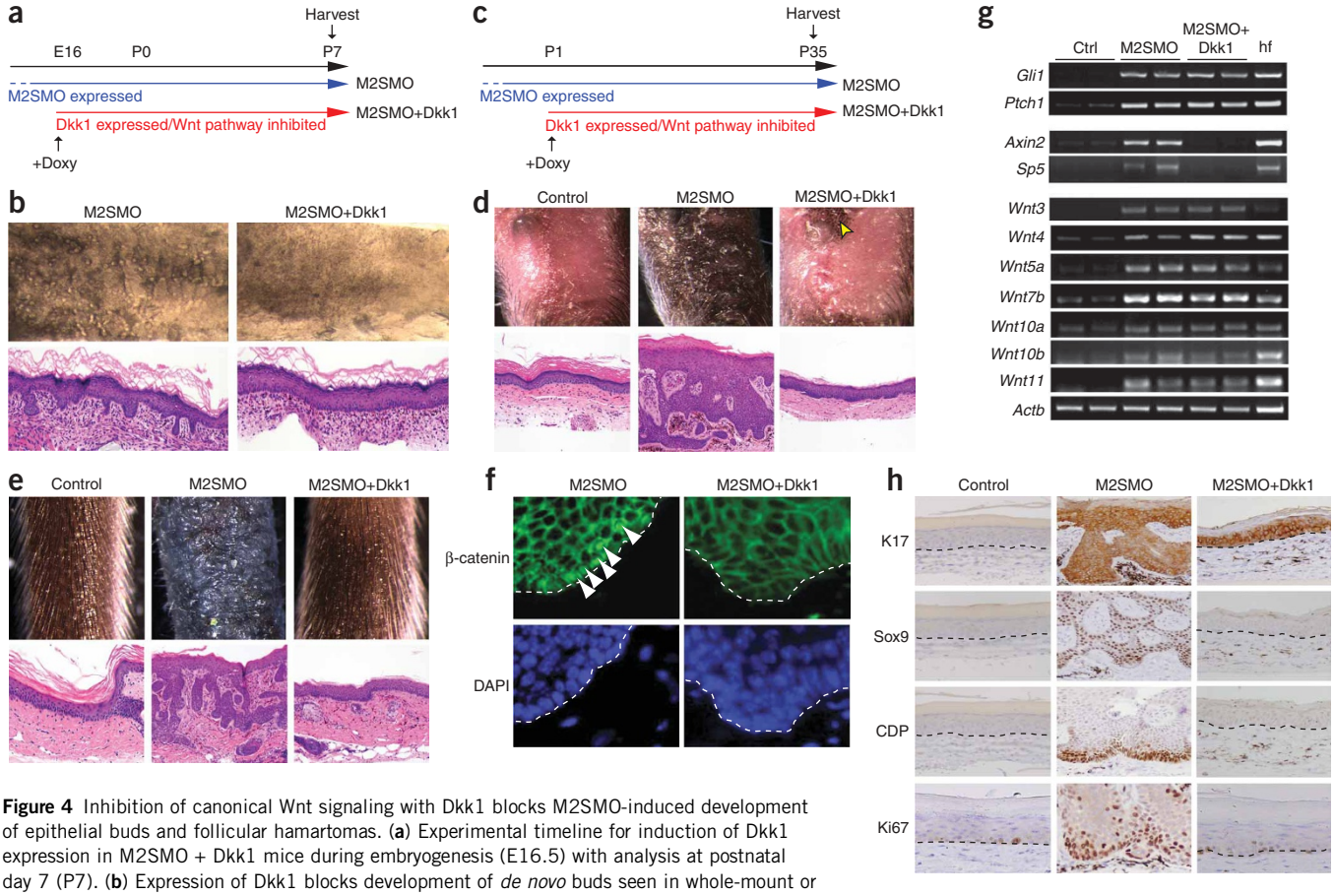

Figure 4 Inhibition of canonical Wnt signaling with Dkk1 blocks M2SMO-induced development of epithelial buds and follicular hamartomas. (**a**) Experimental timeline for induction of Dkk1 expression in M2SMO + Dkk1 mice during embryogenesis (E16.5) with analysis at postnatal day 7 (P7). (**b**) Expression of Dkk1 blocks development of *de novo* buds seen in whole-mount or H&E-stained sections. (**c**) Experimental timeline for Dkk1 induction at P1 with analysis at P35 to assess effects on hamartoma development. (**d**) Gross view and H&E-stained sections of volar skin from control, M2SMO and M2SMO + Dkk1 mice. Note increased pigmentation and hamartoma development in M2SMO skin, as compared with control. The M2SMO-induced phenotype is markedly inhibited by coexpression of Dkk1. Foci of hyperpigmentation were sometimes detected in M2SMO + Dkk1 volar skin near footpads (arrowhead in **d**), and histological examination of these regions revealed buds and/or hamartomas with nuclear β-catenin (not shown), indicating incomplete blockade of canonical Wnt signaling in these regions. (**e**) Gross view and H&E-stained sections of tail skin from control, M2SMO and M2SMO + Dkk1 mice. Note disrupted hair formation, increased pigmentation and hamartomas in M2SMO skin, as compared with control. The M2SMO-induced phenotype is again markedly inhibited by coexpression of Dkk1. (**f**) Immunofluorescence for β-catenin in volar skin. Cells with nuclear β-catenin in M2SMO skin, indicating activation of canonical Wnt signaling, are marked with arrowheads. Inhibition of nuclear β-catenin localization in M2SMO + Dkk1 mice, indicating effective blockade of canonical Wnt signaling. White dotted lines represent epidermal-dermal junction. (**g**) Semiquantitative RT-PCR using RNA from control, M2SMO and M2SMO + Dkk1 tail skin reveals downregulation of *Axin2* and *Sp5* in M2SMO + Dkk1 volar skin, confirming blockade of canonical Wnt signaling. In contrast, expression of Hh target genes *Gli1* and *Ptch1*, as well as Wnt genes, is essentially unaltered in M2SMO + Dkk1 skin as compared with M2SMO skin. (**h**) The Hh-responsive keratin, K17, is not detected in control volar skin, but ectopically expressed in both M2SMO and M2SMO + Dkk1 volar skin, in keeping with sustained activation of Hh signaling in these mice. M2SMO-associated expression of Sox9, CDP and Ki67 are blocked or inhibited in mice also expressing Dkk1.

Taken together, our findings suggest that blockade of canonical Wnt/β-catenin signaling may be a useful strategy for treatment of neoplasms currently considered to be caused by uncontrolled Hh signaling. Because deregulated Hh signaling influences β-catenin signaling primarily at the level of Wnt ligands, the range of potential therapeutic strategies is considerably greater than it is for colorectal and other cancers with mutational defects in APC or β-catenin and would be likely to include antibodies or other recombinant proteins that antagonize the interaction of Wnt ligands with Frizzled and LRP receptors. Future work will better clarify the utility of targeting proximal Wnt pathway components for the prevention or treatment of Hh-dependent neoplasms and other disorders.

METHODS

Transgenic mice and conditional transgene activation. Generation of transgenic mice expressing M2SMO in skin, and triple-transgenic mice expressing M2SMO and doxycycline-inducible Dkk1 expression in skin (*ΔK5-M2SMO; K5-rtTA; TRE-Dkk1*, designated M2SMO + Dkk1), is described in **Supplementary Methods** online. To induce Dkk1 expression in M2SMO + Dkk1 mice, doxycycline (20 mg ml^{-1}) was administered in drinking water with 5% sucrose and in doxycycline-containing chow (Bio-serve, 200 mg/kg). After 3 d mice were maintained on doxycycline-containing chow but received normal drinking water. All mice were housed and maintained according to University of Michigan institutional guidelines, as stipulated by the University Committee on the Use and Care of Animals.

Tissue harvesting and whole-mount preparation. Human superficial BCC cells were obtained from the Cutaneous Surgery and Oncology Unit, Department of Dermatology, University of Michigan Medical School, according to an institutional review board–approved protocol (IRBMED 2000-0015). Embryonic human skin was obtained from Advanced Bioscience Resources. For hematoxylin and eosin (H&E) staining and immunohistochemistry, human and mouse skin samples were fixed in neutral-buffered formalin overnight, transferred to 70% ethanol, processed and embedded in paraffin. Mouse skin was also embedded in OCT Compound (Tissue-Tek) for frozen sections. To prepare whole mounts of volar skin, mice were euthanized and ventral hind limb skin was removed. Volar skin was microdissected and whole-mount preparation was performed essentially as described for tail skin[30]. Transilluminated whole-mount images were captured with a digital camera (Spot RT3; Diagnostic Instruments) mounted on a dissecting stereomicroscope (Leica MZFL3) using Spot Software Version 4.6 (Diagnostic Instruments).

Immunostaining. The following primary antibodies were used for immunostaining: K1 (rabbit polyclonal, 1:1,000; Covance); K5 (rabbit polyclonal, 1:2,000; Covance); K17 (rabbit polyclonal, 1:4,000; gift); β-catenin (mouse monoclonal, 1:1,000; Sigma); Sox9 (rabbit polyclonal, 1:1,000; Chemicon); CDP (rabbit polyclonal, 1:100; Santa Cruz Biotechnology); Ki67 (rabbit polyclonal, 1:500; Vector Laboratories); AE13 (1:10; gift); AE15 (1:50; gift); P-cadherin (rat monoclonal, 1:500; Zymed); E-cadherin (rat monoclonal, 1:1,000; Zymed); cyclin D1 (rabbit polyclonal, 1:1,000; Neomarkers). For immunohistochemistry, 8-μm sections were cut in a parasagittal plane. For all antibodies except AE13, AE15, P- and E-cadherin, immunoreactivity of antigens was restored by immersing slides in boiling 0.01 M citrate buffer, pH ~6, for 10 min. Blocking was performed using 1.5% normal goat serum in phosphate-buffered saline, and tissue sections were incubated with primary antibodies diluted in phosphate-buffered saline containing 1% bovine serum albumin, typically for 1–3 h at room temperature (21–23 °C). Subsequent immunostaining procedures were performed using peroxidase Vectastain ABC kit (Vector Laboratories) and 3,3′-diaminobenzidine as a substrate, according to the manufacturer's protocol. A M.O.M. kit (Vector Laboratories) was used for immunostaining with mouse primary monoclonal antibodies according to the manufacturer's protocol. Sections were counterstained with hematoxylin and mounted using Permount (Fisher Scientific). For immunofluorescence staining, sections were cut from OCT-embedded blocks and fixed in cold acetone for 10 min. Fluorescein isothiocyanate–conjugated secondary antibodies (Jackson ImmunoResearch) were used at 1:75 dilution, and 100 ng ml^{-1} 4-diamidino-2-phenylindole (Merck) was used for nuclear counterstaining. Endogenous alkaline phosphatase activity was visualized using Alkaline Phosphatase Substrate Kit I (Vector Laboratories) and incubating tissue sections with substrate solution for 2–4 h at room temperature.

Immunoblotting. Tissue was homogenized in RIPA buffer (50 mM Tris, pH 7.4, 150 mM NaCl, 1% (v/v) Triton X-100, 0.5 mM EDTA, 1 mM sodium orthovanadate, 200 mM sodium flouride) using a tissue microgrinder (Kontes 749520), vortexed vigorously, cleared by centrifugation for 15 min at 12,000*g* and denatured by heating at 98 °C for 5 min. A 10-μl aliquot of protein extract was resolved on a 10% (w/v) denaturing sodium dodecyl sulfate–polyacrylamide gel (BioRad) and transferred to nitrocellulose membrane. "Activated" β-catenin was detected by probing with α-activated β-catenin (αABC) antibody (mouse monoclonal, 1:1,000; Upstate). Pan-actin antibody (mouse monoclonal, 1:1,000; Labvision) was used to detect actin for loading control. Peroxidase-conjugated secondary antibodies were used and visualized by enhanced chemiluminescence using an ECL Plus kit (Amersham Biosciences).

RNA isolation and semiquantitative RT-PCR. See **Supplementary Methods** and **Supplementary Table 1** online.

Note: Supplementary information is available on the Nature Genetics website.

ACKNOWLEDGMENTS

We thank Pierre Coulombe for providing K17 rabbit polyclonal antibody and Henry Sun for providing AE13 and AE15 antibodies; Eric Fearon and Deb Gumucio for constructive comments on the manuscript; and members of the Dlugosz lab for valuable input on this project. This work was supported by NIH grants R01-AR45973 and R01-CA87837 (A.A.D.), T32-HD007505 and T32-GM07863 (S.H.Y.), and R01-AR47709 and R01-DE015342 (S.E.M.). For production of transgenic mice we acknowledge members of the Transgenic Animal Model Core of the University of Michigan's Biomedical Research Core Facilities, funded in part by P30-CA46592 (University of Michigan Cancer Center Core support).

AUTHOR CONTRIBUTIONS

Experiments were designed by S.H.Y. and A.A.D. Tissue harvests, whole-mount analysis, semiquantitative RT-PCR and immunoblotting were performed by S.H.Y. T.S.W. performed collection of human BCC samples. Immunohistochemistry and immunofluorescence staining were carried out by S.H.Y. and A.W. Genotyping was performed by S.H.Y., A.W., J.L., L.-J.S. and J.F. M2SMO-expressing mice were initially generated by V.G. Animal maintenance and breeding were performed by S.H.Y., A.W., J.L. and J.F. *TRE-Dkk1* mice were provided by T.A. and S.E.M., and *K5-rtTA* mice were provided by A.B.G. T.A. and S.E.M. participated in study design and discussion of the results. The manuscript was written by S.H.Y., with draft revisions by A.A.D. and input from S.E.M. and T.A.

Published online at http://www.nature.com/naturegenetics/
Reprints and permissions information is available online at http://npg.nature.com/reprintsandpermissions/

1. Rubin, L.L. & de Sauvage, F.J. Targeting the Hedgehog pathway in cancer. *Nat. Rev. Drug Discov.* **5**, 1026–1033 (2006).
2. Daya-Grosjean, L. & Couve-Privat, S. Sonic hedgehog signaling in basal cell carcinomas. *Cancer Lett.* **225**, 181–192 (2005).
3. Grachtchouk, V. *et al.* The magnitude of hedgehog signaling activity defines skin tumor phenotype. *EMBO J.* **22**, 2741–2751 (2003).
4. Lever, W.F. Pathogenesis of benign tumors of cutaneous appendages and of basal cell epithelioma. *Arch. Dermatol. Syph.* **57**, 709–724 (1948).
5. Montgomery, H. Histogenesis of basal-cell epithelioma. *Radiology* **25**, 8–23 (1935).
6. Sellheyer, K. & Krahl, D. Basal cell (trichoblastic) carcinoma common expression pattern for epithelial cell adhesion molecule links basal cell carcinoma to early follicular embryogenesis, secondary hair germ, and outer root sheath of the vellus hair follicle: a clue to the adnexal nature of basal cell carcinoma? *J. Am. Acad. Dermatol.* **58**, 158–167 (2008).
7. Huelsken, J., Vogel, R., Erdmann, B., Cotsarelis, G. & Birchmeier, W. β-Catenin controls hair follicle morphogenesis and stem cell differentiation in the skin. *Cell* **105**, 533–545 (2001).
8. Andl, T., Reddy, S.T., Gaddapara, T. & Millar, S.E. WNT signals are required for the initiation of hair follicle development. *Dev. Cell* **2**, 643–653 (2002).
9. Xie, J. *et al.* Activating Smoothened mutations in sporadic basal-cell carcinoma. *Nature* **391**, 90–92 (1998).
10. Fuchs, E. Skin stem cells: rising to the surface. *J. Cell Biol.* **180**, 273–284 (2008).
11. St-Jacques, B. *et al.* Sonic hedgehog signaling is essential for hair development. *Curr. Biol.* **8**, 1058–1068 (1998).

© 2008 Nature Publishing Group http://www.nature.com/naturegenetics

12. Chiang, C. *et al.* Essential role for sonic hedgehog during hair follicle morphogenesis. *Dev. Biol.* **205**, 1–9 (1999).
13. Pasca di Magliano, M. *et al.* Common activation of canonical Wnt signaling in pancreatic adenocarcinoma. *PLoS. ONE* **2**, e1155 (2007).
14. Taipale, J. & Beachy, P.A. The Hedgehog and Wnt signalling pathways in cancer. *Nature* **411**, 349–354 (2001).
15. Mullor, J.L., Dahmane, N., Sun, T. & Altaba, A. Wnt signals are targets and mediators of Gli function. *Curr. Biol.* **11**, 769–773 (2001).
16. Yamazaki, F., Aragane, Y., Kawada, A. & Tezuka, T. Immunohistochemical detection for nuclear β-catenin in sporadic basal cell carcinoma. *Br. J. Dermatol.* **145**, 771–777 (2001).
17. El-Bahrawy, M., El-Masry, N., Alison, M., Poulsom, R. & Fallowfield, M. Expression of β-catenin in basal cell carcinoma. *Br. J. Dermatol.* **148**, 964–970 (2003).
18. Saldanha, G., Ghura, V., Potter, L. & Fletcher, A. Nuclear β-catenin in basal cell carcinoma correlates with increased proliferation. *Br. J. Dermatol.* **151**, 157–164 (2004).
19. Li, X., Deng, W., Lobo-Ruppert, S.M. & Ruppert, J.M. Gli1 acts through Snail and E-cadherin to promote nuclear signaling by β-catenin. *Oncogene* **26**, 4489–4498 (2007).
20. Gat, U., DasGupta, R., Degenstein, L. & Fuchs, E. *De novo* hair follicle morphogenesis and hair tumors in mice expressing a truncated β-catenin in skin. *Cell* **95**, 605–614 (1998).
21. Lo Celso, C., Prowse, D.M. & Watt, F.M. Transient activation of β-catenin signalling in adult mouse epidermis is sufficient to induce new hair follicles but continuous activation is required to maintain hair follicle tumours. *Development* **131**, 1787–1799 (2004).
22. Ito, M. *et al.* Wnt-dependent *de novo* hair follicle regeneration in adult mouse skin after wounding. *Nature* **447**, 316–320 (2007).
23. Jih, D.M. *et al.* Familial basaloid follicular hamartoma: lesional characterization and review of the literature. *Am. J. Dermatopathol.* **25**, 130–137 (2003).
24. Oseroff, A.R. *et al.* Treatment of diffuse basal cell carcinomas and basaloid follicular hamartomas in nevoid basal cell carcinoma syndrome by wide-area 5-aminolevulinic acid photodynamic therapy. *Arch. Dermatol.* **141**, 60–67 (2005).
25. Clevers, H. Wnt/β-catenin signaling in development and disease. *Cell* **127**, 469–480 (2006).
26. Chu, E.Y. *et al.* Canonical WNT signaling promotes mammary placode development and is essential for initiation of mammary gland morphogenesis. *Development* **131**, 4819–4829 (2004).
27. Callahan, C.A. *et al.* MIM/BEG4, a Sonic hedgehog-responsive gene that potentiates Gli-dependent transcription. *Genes Dev.* **18**, 2724–2729 (2004).
28. Mao, B. *et al.* Kremen proteins are Dickkopf receptors that regulate Wnt/β-catenin signalling. *Nature* **417**, 664–667 (2002).
29. Malanchi, I. *et al.* Cutaneous cancer stem cell maintenance is dependent on β-catenin signalling. *Nature* **452**, 650–653 (2008).
30. Braun, K.M. *et al.* Manipulation of stem cell proliferation and lineage commitment: visualisation of label-retaining cells in wholemounts of mouse epidermis. *Development* **130**, 5241–5255 (2003).

© 2008 Nature Publishing Group http://www.nature.com/naturegenetics